

### Stability of marching in time algorithms based on the Electric Field Integral Equation.

*Paul D. Smith*

Department of Mathematics and Computer Science,  
University of Dundee,  
Dundee DD1 4HN,  
Scotland U. K.

Viable approaches to the modelling and numerical computation of the scattering of pulses of electromagnetic energy from a perfectly conducting obstacle, of arbitrary shape, and dimensions not exceeding some number of pulse widths, are based upon either integral equations or Maxwell's (differential) equations. The relative merits of these two approaches are examined in the review [1] by E.K. Miller. We examine solution methods based upon the time dependent form of the Electric Field Integral Equation (EFIE). We note that this equation can be used advantageously to model the transient plane wave response of a body, either open or closed.

The most straightforward way of numerically solving the EFIE is to discretise in space and time in such a way that the surface current density and surface charge density at a particular time  $t$  is expressed as a linear combination of the currents and charges at earlier times  $T < t$ , and the exciting field. Starting with zero initial conditions immediately before the pulse impinges, one can march forward in time to update the current on the body time-step by time-step. With this method it is generally found that numerical instabilities - usually exponentially growing oscillations - swamp the evolving solution (see for example [2]) restricting its usefulness to shorter time scales. In this paper the source of this instability is identified, and a simple technique for eliminating it without loss of accuracy is described. This enables one to use the original marching in time algorithm, slightly modified, with its attendant simplicity.

As a preliminary remark, note that the marching in time algorithm for the related Magnetic Field Integral Equation (MFIE) - which is appropriate for closed bodies only - has been thoroughly analysed in [3] and [4]. The instability was shown to be due precisely to the existence of nontrivial solutions to the frequency domain MFIE, occurring at frequencies at which the interior cavity of the scatterer resonates. The difficulty is easily eliminated by an averaging process [4]. The analysis demonstrates that this is also a cause of instability for the EFIE when applied to closed bodies; in addition since the structure of the discrete approximation is rather like that for a hyperbolic system of partial differential equations, a von Neumann stability analysis reveals another cause of instability.

To illustrate this second cause of instability, consider a simple open structure, a flat rectangular plate  $S$ . Because it is open, the frequency domain EFIE has a unique solution at every frequency (there are no internal resonances), so any source of instability analogous to that found for the MFIE can be ruled out. The EFIE is

$$\mathbf{n} \times \left[ \frac{\partial \mathbf{A}}{\partial t} + \nabla \phi - \mathbf{E}^i \right] = 0 \quad (1)$$

where  $\mathbf{n}$  is the unit normal to the surface  $S$ ,  $\mathbf{E}^i$  is the incident electric field, and  $\mathbf{A}$ ,  $\phi$ , denote the vector and scalar potentials, defined in terms of the induced current  $\mathbf{J}$  and charge  $\rho$  on  $S$ . Here, with  $\mu, \epsilon$  and the speed of light normalised to 1,

$$\mathbf{A}(\mathbf{r},t) = \frac{1}{4\pi} \int_S \frac{\mathbf{J}(\mathbf{r}',t-R)}{R} dS, \quad \phi(\mathbf{r},t) = \frac{1}{4\pi} \int_S \frac{\rho(\mathbf{r}',t-R)}{R} dS \quad (2)$$

where  $R=|\mathbf{r}-\mathbf{r}'|$  denotes the distance between points  $\mathbf{r},\mathbf{r}'$  on  $S$ . The EFIE is supplemented with the continuity equation

$$\nabla_{\circ} \cdot \mathbf{J} + \frac{\partial \rho}{\partial t} = 0 \quad (3)$$

where  $\nabla_{\circ} \cdot \mathbf{J}$  denotes the surface divergence of  $\mathbf{J}$ . As shown in [5], this equation forces the Lorentz gauge condition

$$\frac{\partial \phi}{\partial t} + \nabla \cdot \mathbf{A} = 0 \quad (4)$$

For a flat surface  $S$  in the  $xy$  plane, the vector potential  $\mathbf{A}$  has no component normal to any point of  $S$ , so that (1) relates  $\partial \mathbf{A} / \partial t$  to  $\partial \phi / \partial x$  and  $\partial \phi / \partial y$ ; the divergence operator in (4) coincides with  $\nabla_{\circ}$  on  $S$  in (3).

The solution of this scattering problem consists in solving the EFIE (1) together with either (3) or (4), subject to the edge conditions, which might simply be taken to require that no current flows normally to an edge, or more exactly, the charge - current relation at an edge can be specified, as in [2]. If the first condition is used, the equation pair (1),(3) is easier to use on surfaces with curved edges, as Rynne[6] notes.

The marching in time algorithm may be described as follows. Let the time step be  $\Delta t$ . Suppose the plate lies in the  $xy$  plane in the region  $0 < x < l_x, 0 < y < l_y$ . Divide the plate into  $MN$  smaller rectangles of sides  $\Delta x = l_x/M, \Delta y = l_y/N$ . Several explicit finite difference schemes may now be made from (1) and (4), depending upon whether forward or central differences are used. The surface current is obtained by splitting the potential  $\mathbf{A}$  into two terms  $\mathbf{A}^s + \mathbf{A}^{ns}$ , the first representing the contribution from the rectangle containing the gridpoint  $\mathbf{r}$ , the self-patch contribution, and the second representing the contribution from all the other rectangles. Provided  $\Delta t$  does not exceed  $\Delta x$  or  $\Delta y$ , this enables the current at  $t + \Delta t$  to be approximated in terms of the current at earlier times less than or equal to  $t$ . The algorithm based on (1) and (3) is similar, except that the scalar potential  $\phi$  must be computed from the updated charge (obtained from the equation of continuity) prior to use in the discretised EFIE. The advantage of this second procedure becomes apparent when the surface  $S$  is not flat, and the computation of  $\nabla \cdot \mathbf{A}$  in (4) then involves an awkward integration over surface currents at retarded times (see [2]). However for flat surfaces this disappears.

Let us analyse the stability of one of these finite difference schemes. Set

$$\phi_{mnk} = \phi(m \Delta x, n \Delta y, k \Delta t), \quad A_{mnk}^x = \hat{x} \cdot \mathbf{A}(m \Delta x, n \Delta y, k \Delta t), \quad A_{mnk}^y = \hat{y} \cdot \mathbf{A}(m \Delta x, n \Delta y, k \Delta t),$$

where  $m, n, k$  denote integers or integers plus  $1/2$ . Central differences in time and space yield the scheme (omitting the E-field terms)

$$\begin{aligned} \frac{A_{m,n+1/2,k+1/2}^x - A_{m,n+1/2,k-1/2}^x}{\Delta t} &= - \left[ \frac{\phi_{m+1/2,n+1/2,k} - \phi_{m-1/2,n+1/2,k}}{\Delta x} \right] \quad (m \neq 0) \\ \frac{A_{m+1/2,n,k+1/2}^y - A_{m+1/2,n,k-1/2}^y}{\Delta t} &= - \left[ \frac{\phi_{m+1/2,n+1/2,k} - \phi_{m+1/2,n-1/2,k}}{\Delta y} \right] \quad (n \neq 0) \\ \frac{\phi_{m+1/2,n+1/2,k+1} - \phi_{m+1/2,n+1/2,k}}{\Delta t} &= - \left[ \frac{A_{m+1,n+1/2,k+1/2}^x - A_{m,n+1/2,k+1/2}^x}{\Delta x} + \frac{A_{m+1/2,n+1,k+1/2}^y - A_{m+1/2,n,k+1/2}^y}{\Delta y} \right] \end{aligned}$$

Here  $0 \leq m < M, 0 \leq n < N$  except as stated. Note that  $A_{0,n+1/2,k+1/2}^x, A_{m+1/2,0,k+1/2}^y, A_{M,n+1/2,k+1/2}^x$  and  $A_{m+1/2,N,k+1/2}^y$  are determined by the boundary conditions. This scheme of spatially staggered grid points has been used previously in the frequency domain [7]. To ascertain stability we set  $(A_{mnk}^x, A_{mnk}^y, \phi_{mnk}) = \xi^k e^{jm\alpha\Delta x + jn\beta\Delta y} (a, b, c)$ , where  $(a, b, c)$  is an arbitrary vector (see [8]). The resulting matrix eigenvalue equation shows that  $\eta = j\xi$  is a root of

$$\eta^2 \pm 2\Delta t \eta \sqrt{\frac{\sin^2 \alpha \Delta x / 2}{(\Delta x)^2} + \frac{\sin^2 \beta \Delta y / 2}{(\Delta y)^2}} + 1 = 0.$$

To avoid instability  $|\eta|$  must not exceed 1, i.e.  $\Delta t < 1/\sqrt{(\Delta x)^{-2} + (\Delta y)^{-2}}$ ; in the sequel  $\Delta x = \Delta y = \Delta$ , so this means  $\Delta t < \Delta/\sqrt{2}$ . It is clear that the same stability criterion applies if the equations (1) and (3) are used: this was numerically verified in the examples below.

To illustrate this criterion, consider a square plate of side 2 units, struck at normal incidence by a Gaussian pulse of profile  $\exp(-z^2)$ , with E-field parallel to plate edge. The backscattered farfield response is shown in Fig. 1. The values are in total agreement with those in [2], until the instability sets in (as it also does in [2]). The instability is expected in this case since  $\Delta t/\Delta$  exceeds  $1/\sqrt{2}$ . It disappears when this ratio is reduced below  $1/\sqrt{2}$ , as shown in Fig. 2. Fig. 3 shows, on a much longer time scale, the logarithmic modulus of the solutions graphed in Figs. 1 and 2, and confirms that the envelope of the instability grows exponentially as expected in the unstable regime, but in the stable case decays exponentially at late time to a level fixed by machine accuracy. Note that Bennett's results [2] are computed with  $\Delta t/\Delta = 0.8$  and the late time instability is attributable to violation of the stability criterion. (In [2] a single equation is obtained for the potential  $A$  from (1) after elimination of  $\phi$  via (4); von Neumann stability analysis of its discretisation yields the identical stability criterion.)

Now consider two identical square plates parallel, edges aligned, of side and separation 1 unit, illuminated in this way. Although the time step is chosen sufficiently small, instability is observed in the backscattered farfield response, normalised by distance (Fig. 4). This is due to the existence of SEM poles with small real part for such a system. As a pair of parallel plates are brought closer and closer, a lightly damped transmission line mode is supported and some poles of the structure approach the imaginary axis. This phenomenon is a feature of two element transmission line systems: see for example [9]. The discretisation process effectively displaces some poles into the right half plane. The cure is precisely that prescribed in [4], consisting of a running average over 3 time steps. The stabilised result is shown in Fig. 5. The longer time logarithmic plot of Fig. 6 confirms the effectiveness of the technique.

To summarise, the marching in time technique applied to the EFIE requires that  $\Delta t < \min(\Delta x, \Delta y)$  in order to get an explicit scheme for updating the potential and surface current values at each time step; in order to obtain a stable scheme a von Neumann stability analysis shows that the time step must not exceed  $1/\sqrt{(\Delta x)^{-2} + (\Delta y)^{-2}}$ . For structures which do not possess SEM poles near the imaginary axis this is sufficient to produce a stable method; otherwise the previously reported averaging technique [4] must be applied to get a stable scheme. The analysis is valid for other planar structures (e.g. disks) and is expected to apply approximately to surfaces with curvature in one direction (e.g. cylinders), since finite differences can be utilised [7].

**Acknowledgement.** The author acknowledges many useful discussions with Dr. B. P. Rynne and his helpful assistance in preparing the diagrams.

#### References.

- [1] E. K. Miller (1988) *IEEE Trans. Antennas Propagat.* AP- 36 ,1281-1305.
- [2] C. L. Bennett, H. Mieras (1981) *Radio Science* 16 ,1231-1239.
- [3] B. P. Rynne (1985) *IMA J. Applied Math.* 35 ,297-310.
- [4] P. D. Smith (1988) *Bull. IMA* 24 ,166-170.
- [5] D. S. Jones (1964) *Theory of Electromagnetism.* (O.U.P).
- [6] B. P. Rynne (1986) *M.O.D. Research Report 5, Uni. of Dundee.*
- [7] A. W. Glisson, D. R. Wilton (1980) *IEEE Trans. Antennas Propagat.* AP- 28 ,593-603.
- [8] A. R. Mitchell, D. F. Griffiths (1980) *The Finite Difference Method in Partial Differential Equations.* (Wiley).
- [9] K. R. Umashankar, T. H. Shumpert, D. R. Wilton (1980) *IEEE Trans. Antennas Propagat.* AP- 23 ,178-184.

Copyright (c) Controller HMSO London 1989.

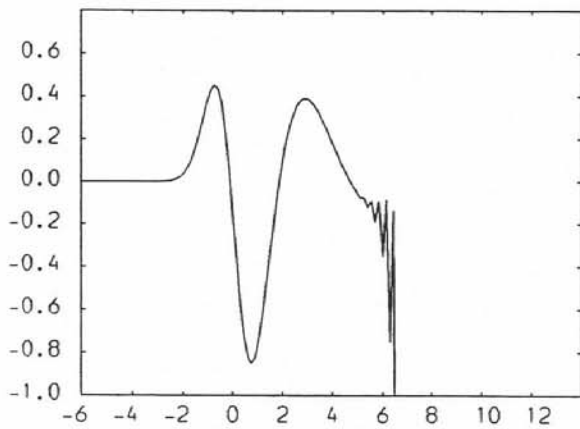


Fig.1

Square plate backscattered E-field,  $\Delta t/\Delta = 0.75$ .

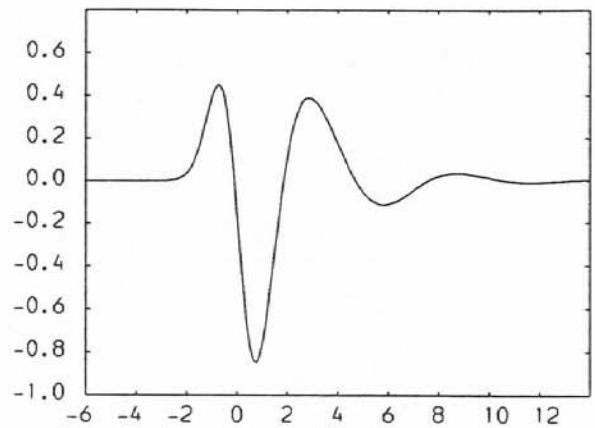


Fig.2

Square plate backscattered E-field,  $\Delta t/\Delta = 0.65$ .

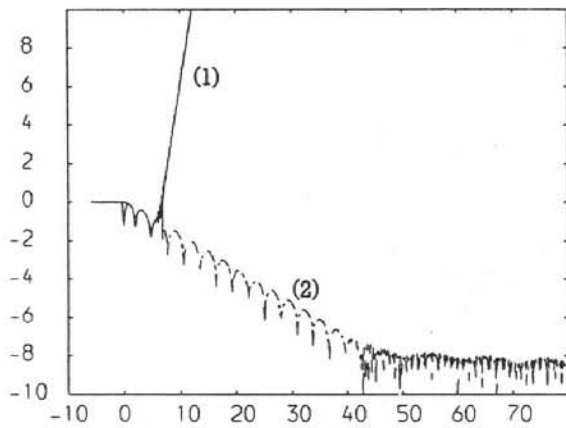


Fig.3

Logarithm of backscattered E-fields in figs.1,2.

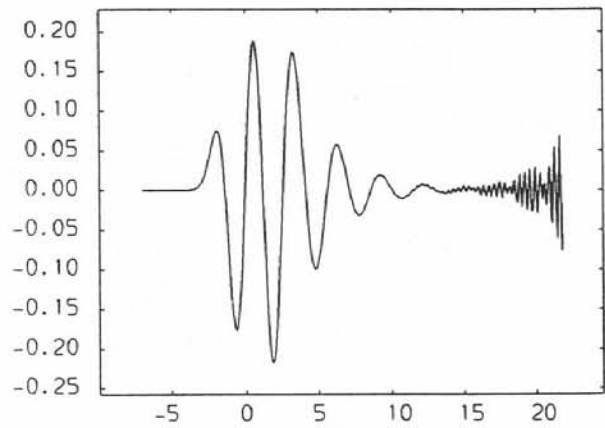


Fig.4

2 Square plates: backscattered E-field,  $\Delta t/\Delta = 0.6$ .

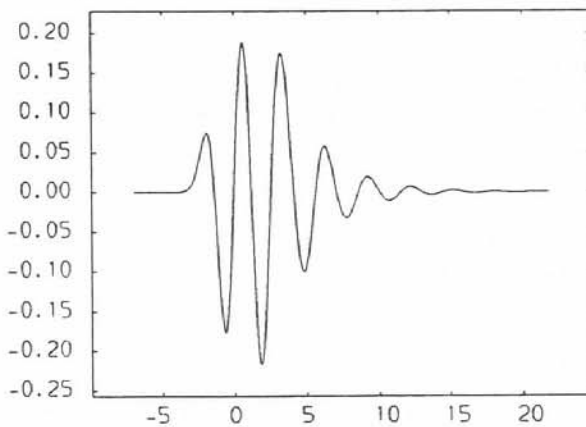


Fig.5

2 Square plates: stabilised by running average.

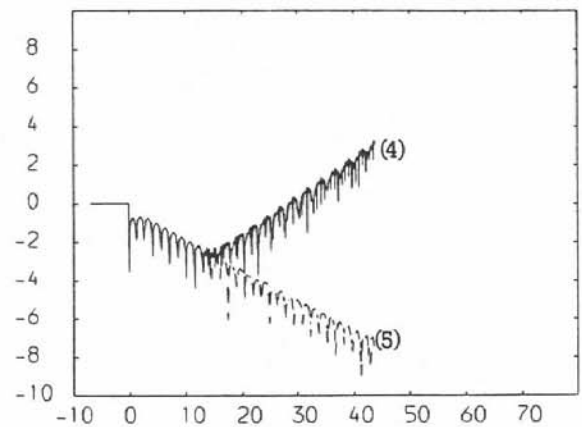


Fig.6

Logarithm of backscattered E-fields in figs.4,5.